DESIGN REVIEW AND ANALYSIS FOR A PRATT & WHITNEY FLUID-FILM BEARING AND SEAL TESTING RIG

FINAL REPORT

Prepared for NASA George C. Marshall
Space Flight Center

Contract Number: NAG8-294

by
Dara W. Childs
Turbomachinery Laboratory
Texas A&M University

November 3, 1994

ABSTRACT

A design review has been completed for a Pratt & Whitney (P&W)-designed fluid-film-bearing and annular-seal test rig to be manufactured and installed at George C. Marshall Space Flight Center (MSFC). Issues covered in this study include

(a) The capacity requirements of the drive unit.
(b) The capacity and configuration of the static loading system.
(c) The capacity and configuration of the dynamic excitation system.
(d) The capacity, configuration, and rotordynamic stability of a test bearing, support bearings, and shaft.
(e) The characteristics and configuration of the measurement transducers and data channels.

This study was initiated by a review of a complete drawing set and operating conditions provided by P&W. The results of the initial review were reported to NASA-MSFC and P&W representatives on 8 October 1993. Based on this review, various changes were made in the drawings and proposed operating conditions. The present report is based on the updated data.

A review of the presently proposed hardware and operating conditions shows a basically sound design. The apparatus should be able to measure the static characteristics of proposed hydrostatic bearings. The largest uncertainty in the ability to identify rotordynamic characteristics concerns the dynamic characteristics of the motion transducers. **Assuming that the motion transducers work as predicted, in a cryogenic environment,** the apparatus should also work satisfactorily for parameter identification of rotordynamic coefficients.

Meaningful uncertainty characteristics for the complete system can not be made without accurate measurements of phase uncertainty for all components of the measurement system, particularly the displacement transducers. Phase data are not available for the motion transducers; hence, uncertainties can only be roughly estimated. By assuming that all components of the measuring system are at least as accurate as comparable systems in the currently operating system at Texas A&M University (TAMU), uncertainty estimates are provided by extrapolating TAMU measured results to higher pressures and speeds. The projected uncertainty results are generally comparable to TAMU experience and are marginally better in some cases.

A new issue raised in this report concerns the consequence of a displacement of the mass center of the test bearing assembly from the lines of action of the applied dynamic loads. The mass center offset causes a pitching and yawing excitation of the bearing assembly about the mass center. As a consequence, point contacts between the outer radius of the assembly and the parallel guiding surfaces will occur during excitation, aggravating the

uncertainty due to Coulomb damping forces. Also, the pitching and yawing motion introduces an error into the transducer-motion measurements. An error on the order of 4% is predicted at the high-pressure and high-speed condition. This problem is not overwhelming but it could and should be eliminated by a redesign which will eliminate the offset.

Various issues remain unresolved by the authors of this report; viz., local deflections of the hollow shaft due to pressure loading, phase-response characteristics of the motion transducers at cryogenic temperatures, and the effectiveness and correctness of the Zonic "box" and software which will be used for parameter identification.

DESIGN REVIEW AND ANALYSIS FOR A PRATT & WHITNEY FLUID-FILM BEARING AND SEAL TESTING RIG

TABLE OF CONTENTS

INTRODUCTION

Pratt and Whitney (P&W) is in the process of developing a cryogenic tester to identify the static and dynamic characteristics of high-speed hydrostatic bearings. This report summarizes the results of a review and analysis of their design.

The initial review of the P&W design was based on data provided by P&W, consisting of a complete set of drawings plus specifications of operating conditions, instrumentation, etc. A presentation of initial findings was made to NASA-MSFC and P&W personnel on 8 October 1993. Issues raised at this meeting were reviewed by NASA-MSFC and P&W personnel, and a subsequent set of revised drawings were developed and forwarded by P&W. The initial review was carried out for an LH_2 bearing with supply pressures out to 5000 psi and running speeds to 80,000 rpm. At NASA's request, the present review was for a typical LO_2 bearing design using LO_2 and LN_2, speeds to 30,000 rpm and supply pressures to 2000 psi.

The contents of this report are organized on a design "issue" basis, with each point of concern stated and then reviewed as to status and disposition. Most of the points covered here were raised in the 8 October 1993 meeting.

EXTRANEOUS LOAD PATHS

Measurement of the static load-deflection characteristics of a bearing, and identification of rotordynamic coefficients for small motion about an equilibrium position are central research objectives involved in the tester. Static and dynamic loads are to be applied **to the bearing**, and the resultant static and/or dynamic deflections are to be measured. Alternative load paths from the bearing/loader assembly to "ground" mean that the specified load used in identification is in error, and the resultant measured properties are also in error. The contents of this section consider various extraneous load paths which have the potential for introducing errors into measured results.

Figure 1 illustrates the initial dynamic load-path design. The dynamic load should be transmitted from a hydraulic shaker head to the bearing-support structure and thence to the test bearing itself. The bearing-support structure is guided between two parallel surfaces but is otherwise not constrained in the axial direction. The initial design presents the following alternate load paths between the exciter head (where the input force is measured) and the test bearing:

(a) Shaft seal around the exciter-shaft bore,

(b) Stationary seals between the bearing-support structure and the test housing,

(c) Fluid-film forces between the outer circumference of the bearing-support structure and the inner circumference of the test housing,

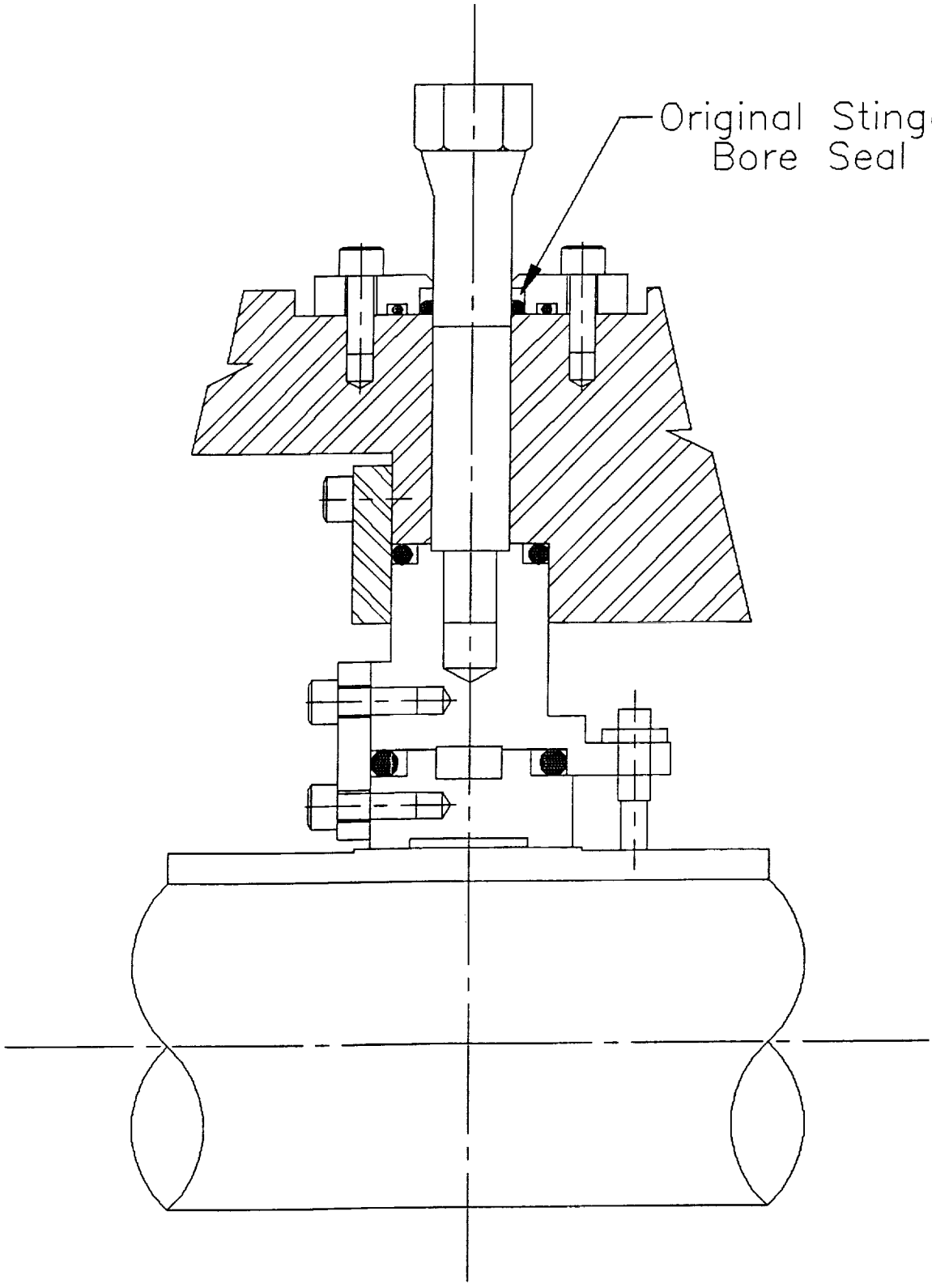

1. Original dynamic loader design

(d) Reaction forces from the static loader perpendicular to the excitation force,

(e) Reaction forces from the static loader parallel to the excitation force, and

(f) Coulomb-friction forces at the parallel faces between the bearing-support structure and the housing.

A discussion of these individual extraneous load paths and their impact on measurement accuracy follows.

Shaft Seal Around Exciter-Shaft Bore

Figure 2 illustrates P&W's redesign which eliminates this seal and its associated problems.

Stationary Seal Between the Bearing Support Structure and the Test Housing

The redesign of figure 2 does not change these seals. The difficulty with these load elements is that their load-deflection characteristics are clearly a function of the pressure level that is sealed against. Hence, a "dry shake" test at reduced or zero supply pressure can not be used to calibrate or eliminate their influence. The argument can be made that these seals are "soft" elements in comparison to the bearing load paths, and their modification of the imposed load should be small. This argument may be correct, but the presently planned test program will not address the uncertainty involved in this problem. The uncertainty could be eliminated by plugging the bearing orifices and conducting a dryshake test with the system pressurized with gaseous nitrogen over the operating pressure range of the system.

Fluid-Film Forces Developed at the Annulus Between the Bearing-Support Structure and the Housing

This issue concerns forces developed by squeeze-film action at this annular interface. The low viscosity of LO_2 or LN_2 should yield reduced or minimal viscous forces; however, tests with squeeze-film dampers at TAMU have shown significant added-mass terms at enlarged clearances. P&W has moved to reduce this force by increasing the radial clearance from C_r=.025/.031 in to C_r=.055/.061 in the new design. A dryshake test of the system with the bearing flooded but not pressurized will provide a good measure of any added-mass contribution from this annulus.

Load Sharing from the Static Loader Perpendicular to the Dynamic Load Excitation

Figures 3 and 4 illustrate the original and modified designs of the connection between the static loader (pneumatic load cylinder) and the test-bearing support structure. The initial concern was that a significant portion of the dynamic load applied perpendicular to a static loader would be absorbed by the static loader. P&W's modified design has a greatly reduced

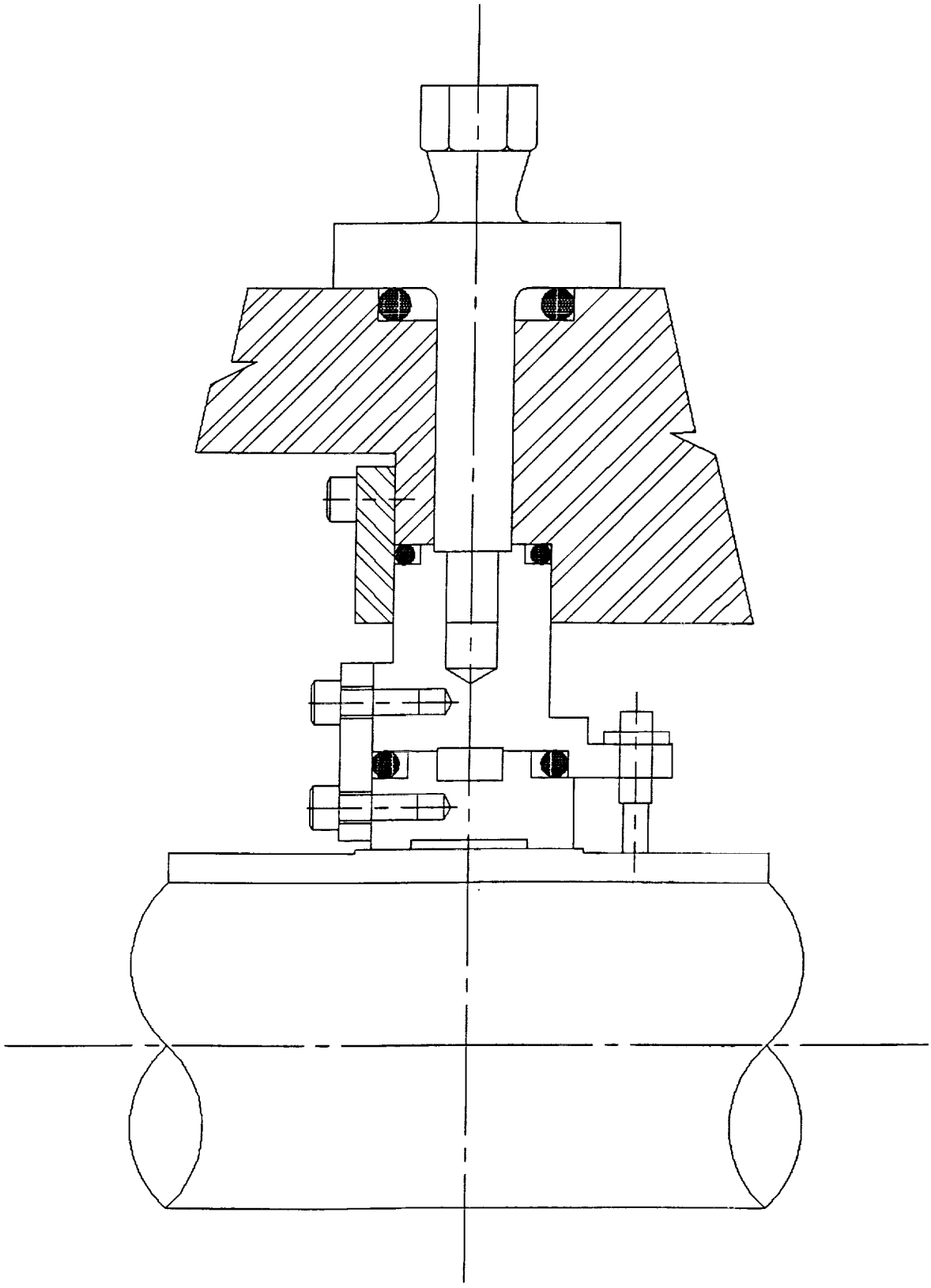

2. Modified dynamic loader design

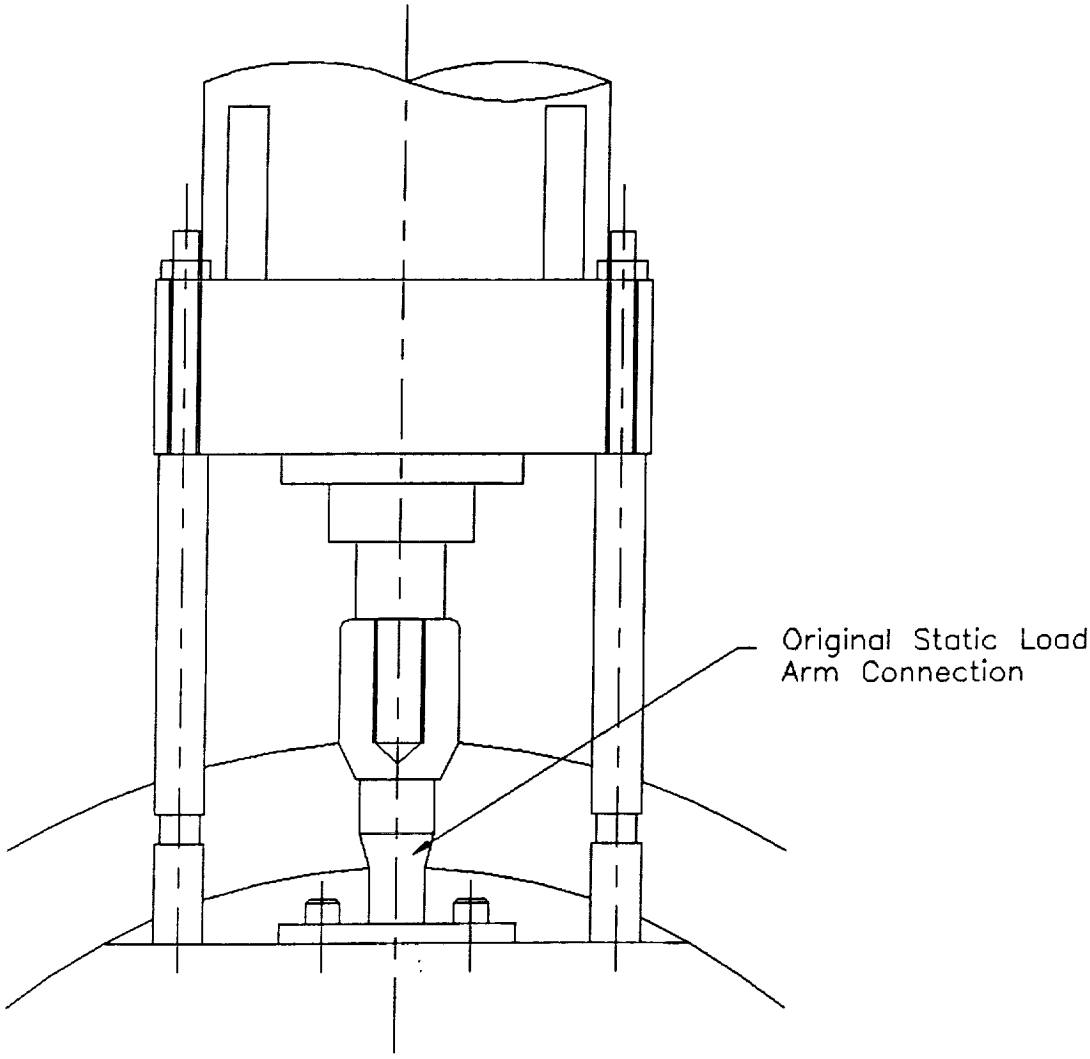

3. Original static loader configuration

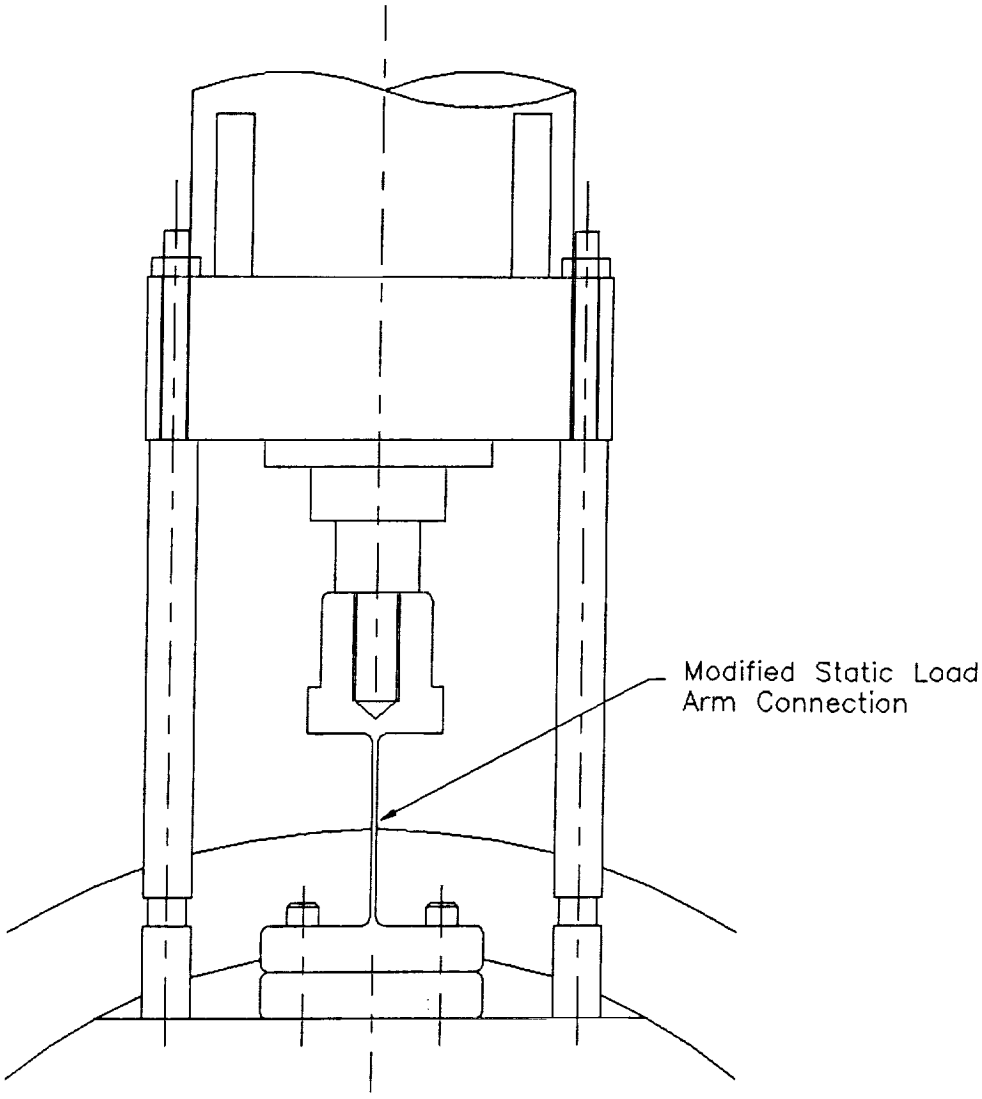

4. Modified static loader configuration

bending moment of inertia on the static loader connection, which should substantially eliminate this potential problem by reducing the stiffness of this alternate load path.

Load Sharing from the Static Loader Parallel to the Dynamic Load Excitation

The concern on this point was that the static loader was directly and firmly tied into the test-bearing assembly; hence, the stiffness and damping of the static loader would be measured as part of the dynamic characteristics of the bearing. Our review of the characteristics of the loader from manufacturer's specifications eliminated this concern. Specifically, the stiffness and damping characteristics of the static loader are insignificant compared to the bearing characteristics.

Coulomb Damping

An axial pressure differential across the test bearing can generate an axial thrust load which would cause the bearing support structure to come into contact with parallel guide surfaces of the test section outer wall. Motion of the bearing relative to the wall would then give rise to Coulomb friction forces which would introduce errors into the rotordynamic-coefficient identification procedure. At the 8 October 1993 meeting, predictions were presented for an LH_2 bearing with a 2 psi axial pressure drop across the bearing and a range of Coulomb friction factors out to 0.1. P&W representatives stated that there would be zero axial ΔP across the bearing based on downstream flow characteristics, and (if required) they would put a hole through the bearing support structure to guarantee that the ΔP is zero. This step obviously eliminates axial thrust due to pressure differential; however, the test shaft is vertical, and the weight W_s must still be reacted by contact forces. NASA MSFC officials requested that the analysis be repeated for LO_2 and LN_2 bearings with Coulomb friction coefficient μ extended out to 0.2.

The analysis of Coulomb-friction effects is based on the following equations of motion for the test bearing and its support mass M_s

$$\left(\begin{bmatrix} M_{XX} & M_{XY} \\ M_{YX} & M_{YY} \end{bmatrix} + \begin{bmatrix} M_s & O \\ O & M_s \end{bmatrix} \right) \begin{Bmatrix} \ddot{X} \\ \ddot{Y} \end{Bmatrix} + \begin{bmatrix} C_{XX} & C_{XY} \\ C_{YX} & C_{YY} \end{bmatrix} \begin{Bmatrix} \dot{X} \\ \dot{Y} \end{Bmatrix} + \begin{bmatrix} K_{XX} & K_{XY} \\ K_{YX} & K_{YY} \end{bmatrix} \begin{Bmatrix} X \\ Y \end{Bmatrix} = \begin{Bmatrix} fs_x \\ fs_y \end{Bmatrix} + \begin{Bmatrix} fq_x \\ fq_y \end{Bmatrix} + \begin{Bmatrix} fn_x \\ fn_y \end{Bmatrix} \quad (1)$$

The equations of motion have been rearranged by taking the forces due to stiffness, damping, and mass matrices for the bearing to the left hand side of the equation. The force

components on the right hand side are fs_x, fs_y (actual measured excitation forces from a selected TAMU water-bearing test), fn_x, fn_y (random forces), and fq_x, fq_y (Coulomb friction forces). The random force components are defined by

$$\begin{aligned} fn_x &= RND(10)\cos[RND(2\pi)] \\ fn_y &= RND(10)\sin[RND(2\pi)] \end{aligned} \tag{2}$$

where RND(X) is a random number between 0 and X. The result is band limited between 40 440 Hz.

The Coulomb friction force vector has a magnitude of μW_s and a direction opposite to the bearing's velocity. Its components are defined by:

$$\begin{aligned} fq_x &= -\mu W_s \cos\theta \\ fq_y &= -\mu W_s \sin\theta \\ \tan\theta &= \dot{Y} / \dot{X} \end{aligned} \tag{3}$$

The test bearing characteristics and operating conditions are taken from Pelfrey (1993) as relayed via FAX from Howard Gibson to Keith Hale on 24 November 1993. Pelfrey's results are based on predictions from San Andres' TAMU codes. We were not provided Pelfrey's complete input data files; however, by iterating the missing input data we obtained the same calculated results. Calculated rotordynamic coefficients are used for stiffness, damping, and mass coefficients of Eq.(1).

The impact of Coulomb friction forces on parameter identification is determined by operating Eq.(1) as a simulation model. The differential equation is integrated using zero initial conditions with continuous excitation from **fs, fq**, and **fn**. Output values for X(t), Y(t), $\ddot{X}(t)$, $\ddot{Y}(t)$, and input values $fs_x(t)$, $fs_y(t)$ are retained. The "unknown" stiffness, damping, and inertia coefficients are identified using the parameter identification procedure of Rouvas and Childs (1993).

The weight of the bearing and stator is 23.5 lbs. Figure 5 shows the influence of Coulomb friction forces and noise on the identification process for the test bearing using LN_2 as a test fluid. The results are for operation at 30,000 rpm with supply pressures of 1000 and 2000 psi. The bearing is centered for all test cases. For μ=0, the values shown are very close to the input-data values, although noise input causes slight differences between M_{XX} and M_{YY} and significant differences between M_{XY} and $-M_{YX}$. As μ is increased, the identified parameters move away from the correct, input values. Figure 6 shows the percentage change in rotordynamic coefficients due to Coulomb friction. The results of figures 5 and 6 show that Coulomb friction makes a tiny change in the direct and cross-coupled stiffness, a

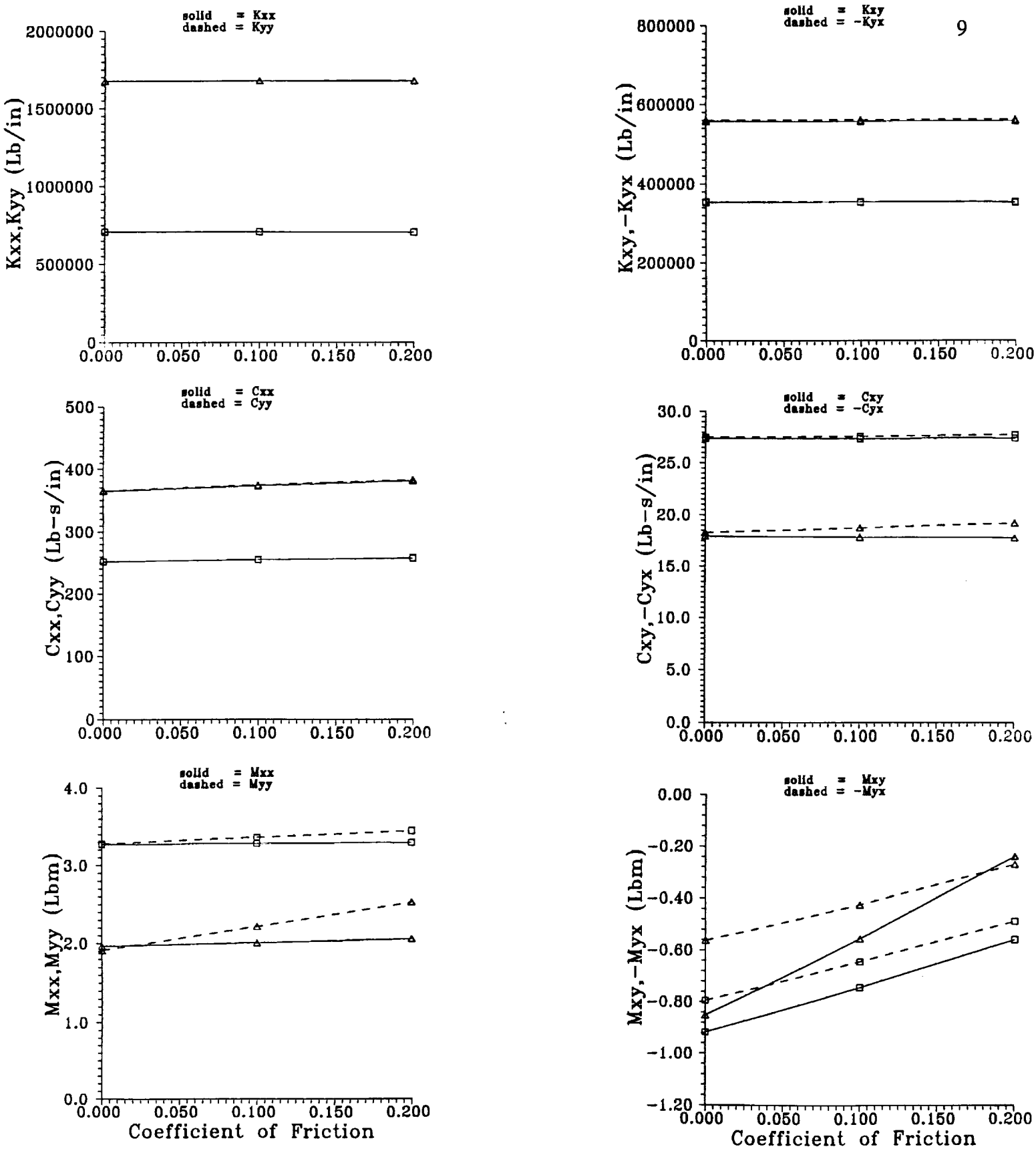

5. Identified rotordynamic-coefficients for the test bearing with LN_2 as a test fluid

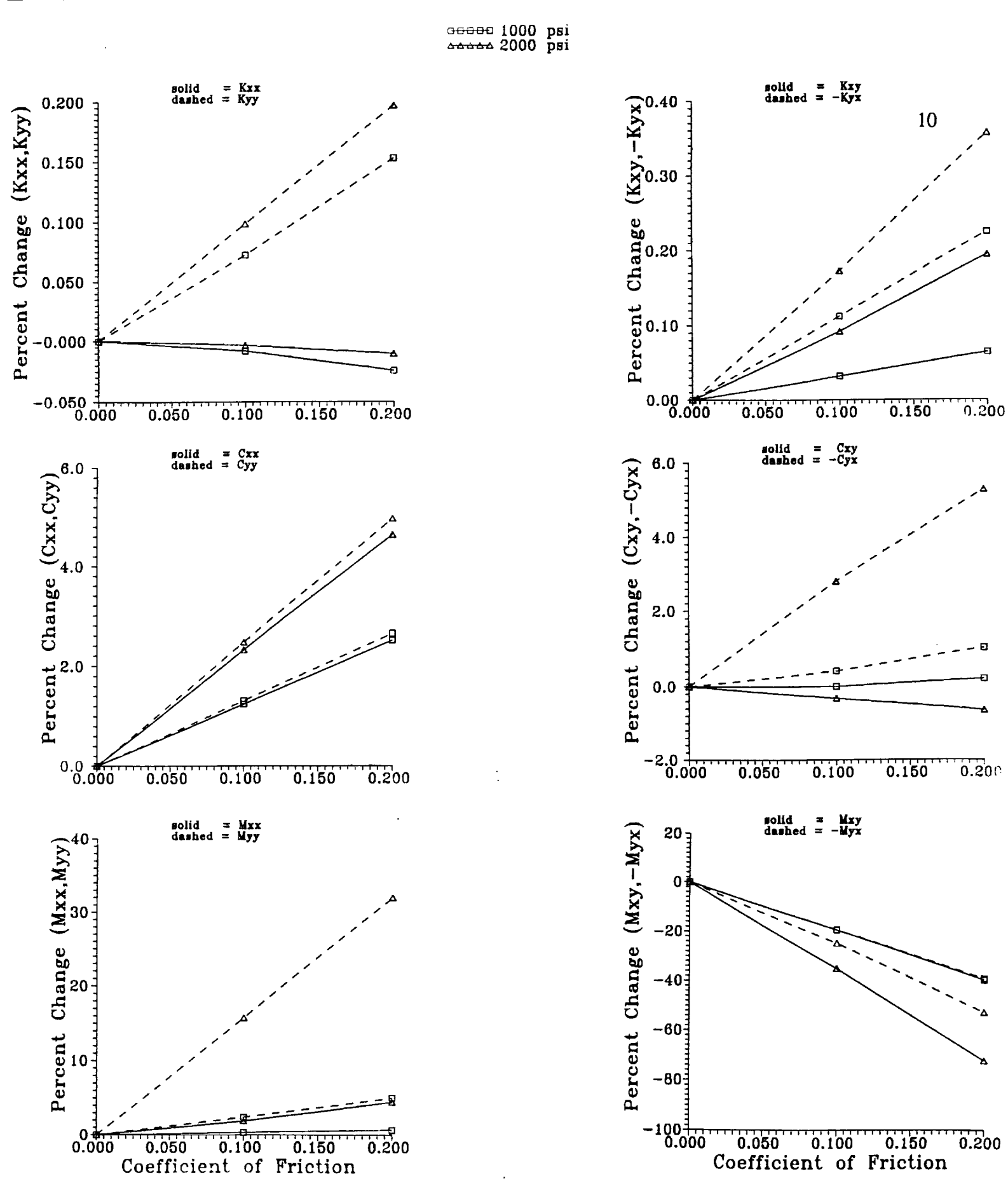

6. Percentage change in rotordynamic coefficients due to Coulomb friction with ω = 30,000 rpm and LN_2 used as the test fluid

perceptible but small change in direct and cross-coupled damping, and a major change in the mass coefficients. Comparable results are shown in figures 7 and 8 when LO_2 is the test fluid. The impact of Coulomb friction in the present LO_2 and LN_2 bearing operation is much lower than earlier results (for the LH_2 bearing), because the present bearings have significantly larger rotordynamic-coefficient magnitudes.

The errors introduced by Coulomb friction can not be "calibrated out." They represent a permanent precision error in parameter identification of rotordynamic coefficients. Coulomb-friction could be eliminated by using hydrostatic centering pads to axially center the bearing support structure.

Another **potential** problem which could be eliminated by centering pads concerns moment excitation of the test-bearing assembly. The mass center of the test-bearing assembly is not colinear with the input excitation force axis. Hence the excitation force will yield an unwanted pitching or yawing moment on the bearing assembly simultaneously with the excitation force. Analysis covering this point is provided in the Rotordynamic Issues section.

OPERATIONAL CONCERNS

With regard to operational concerns, the following questions were raised in the 8 October meeting:

(a) How much power will be required by the turbine to overcome the drag torques of the slave bearings and the test bearing?

(b) What flowrate is required?

(c) How does the clearance in the bearings vary with speed, and is interference possible at elevated speeds?

(d) Will the shakers provide an adequate force and frequency range for parameter identification?

Power Requirements

Calculated power requirements for the system of two slave bearings and one test bearing at 30,000 rpm are:

$$\begin{aligned} LO_2: &\quad PWR = 68.3 \quad HP = 50.9 \quad KW \\ LN_2: &\quad PWR = 44.3 \quad HP = 33.0 \quad KW \end{aligned} \tag{4}$$

P&W has previously demonstrated power capability in excess of this requirement.

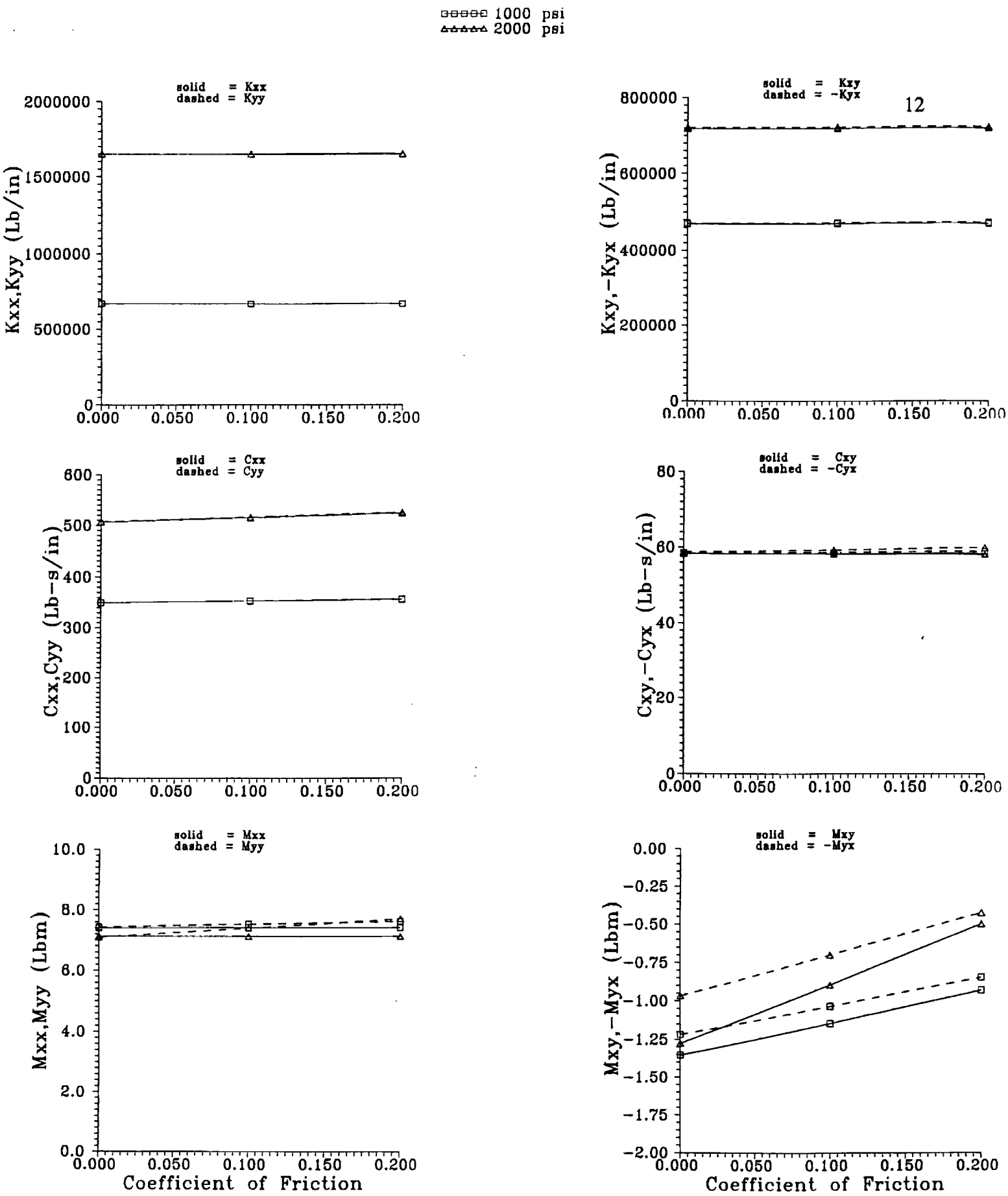

7. Identified rotordynamic-coefficients for the test bearing with LO_2 as a test fluid

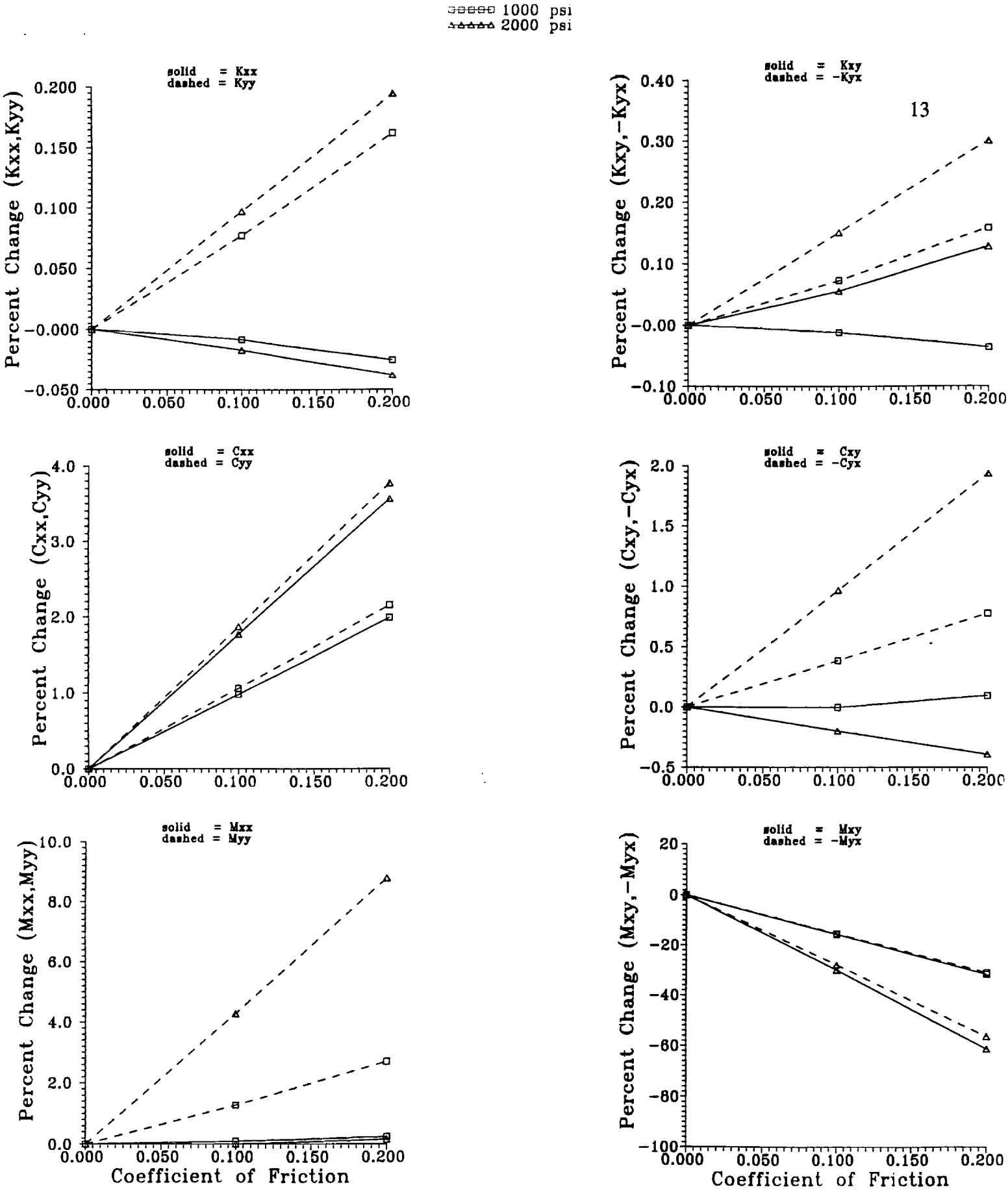

8. Percentage change in rotordynamic coefficients due to Coulomb friction with ω = 30,000 rpm and LO_2 used as the test fluid

Flowrate Requirements

Concerning flowrate requirements, at 30,000 rpm with 1500 psi supplied to the slave bearings and 2000 psi supplied to the test bearings, the requirements are:

$$\begin{aligned} LO_2: &\quad \dot{M} = 3.26 \ \ Kg/sec = 7.18 \ \ lb/sec \\ LN_2: &\quad \dot{M} = 2.80 \ \ Kg/sec = 6.16 \ \ lb/sec \end{aligned} \tag{5}$$

NASA officials must judge the adequacy of the MSFC system for meeting these calculated flowrate requirements.

Interference and Rub Due to Shaft Growth

Concerning the possibility of interference due to shaft growth, the initial study using an 80,000 rpm upper speed limit showed an interference condition at around 74,000 rpm (starting from .004 in radial clearance). The reduced upper speed limit of 30,000 rpm eliminates this problem.

Excitation Frequency Requirements

The initial upper speed limit of 80,000 rpm (1333 Hz) caused an identification problem with the shaker heads, which have a sharply reduced force capacity at frequencies approaching 1000 Hz. The Zonic shakers proposed for use will work very well for the current 0-30,000 rpm (0-500 Hz) frequency range.

Static-Load Requirements

An issue which was not raised during our earlier discussions concerned the static load capacity of the tester. The question to be addressed is simply: What static eccentricity can be achieved using the loaders? Based on the manufacturer's recommendation, the static load capacity of the pneumatic cylinders is 2500 lb (11.2 KN) in a push mode and 2350 lbs (10.6 KN) in a pull mode. These values are obtained with an assumed 250 psi supply pressure and an upper operation limit of 75% capacity, based on the manufacturer's recommendation. Applying a pull load of 2350 lbs to the test bearing in the X direction with a supply pressure of 2000 psi and a running speed of 30,000 rpm yielded the following predicted static eccentricities:

$$\begin{aligned} LN_2: &\quad \epsilon_{xo} = .456, \quad \epsilon_{yo} = .166, \quad \epsilon_o = .646 \\ LO_2: &\quad \epsilon_{xo} = .424, \quad \epsilon_{yo} = .201, \quad \epsilon_o = .600 \end{aligned} \tag{6}$$

These eccentricity results are for a nominal radial clearance of .003 in. A judgement of the adequacy of these predicted results can only be made by NASA-MSFC. Obviously, larger static eccentricities can be obtained by using both the X and Y loaders simultaneously. Also, the user could decide to exceed the manufacturers recommended limit of 75% of rated capacity. Tests at TAMU have routinely covered the zero to 0.5 eccentricity-ratio range for ϵ_{xo} with dynamic excitation about the static eccentricity points.

STRUCTURAL CONCERNS

Our initial review of the tester raised one concern; namely, pressure within the recesses could cause perceptible local deflections of the hollow shaft. A crude calculation showed that the shaft diameter could be reduced by 0.45×10^{-3} in with a supply pressure of 5000 psi and a pressure ratio of 0.6 (3000 psi recess pressure). In addition, the recess pressures caused a circumferential variation of 0.05×10^{-3} in. At 60,000 rpm, the radial clearance was predicted to be 1.40×10^{-3} in without local deflections; hence, the local deflections were roughly one third of the operating clearance. Our concerns were: (a) the local deflections could not be accounted for in the predictions of hydrostatic-bearing performance, and (b) the results could not be extrapolated to turbopumps using solid shafts. The impact of local deflections has been substantially reduced by the reduction in supply pressure to 2000 psi and a reduction in running speed to 30,000 rpm. The predicted local deflection is now 0.23×10^{-3} in versus a nominal clearance of 3.5×10^{-3} in. Hence the local deflection could amount to roughly 7% of the nominal clearance. Only NASA MSFC officials can decide whether this issue merits further consideration in terms of developing an accurate finite-element prediction of the deformed surface of the shaft.

ACCURACY CONCERNS

The following issues were raised during our October discussions:

(a) The accelerometers are mounted via a cantilever arrangement on the dynamic load assembly. We prefer a direct in-line attachment.

(b) The motion transducer is mounted on a cantilever structure attached to the test-bearing assembly. We recommended a closer and more direct mounting arrangement to reduce the impact of fluid-flow excitation.

(c) The static pressure connections to the bearing recesses provide a capacitance coupling to the recesses which can substantially modify the rotordynamic characteristics of the bearing. Goodwin et al. (1988) deliberately introduced

capacitance to bearing recesses to change the rotordynamic characteristics. This problem was eliminated at TAMU by using close-coupled dynamic pressure transducers.

P&W officials reviewed points (a) and (b) and concluded that the natural frequencies of the accelerometers and motion transducer assemblies were adequately elevated above the input excitation frequencies. We (TAMU) have not been informed as to the resolution of the capacitance issue.

IDENTIFICATION CONCERNS

A review of the hardware and software selected by P&W for identification of rotordynamic coefficients was not a responsibility of this study. However, we forwarded dynamic data from our tester to NASA MSFC (Howard Gibson) on 10 December 1993 for use in demonstrating the effectiveness of the identification system. The data we forwarded was digitized. We were informed that the Zonic "box" selected for parameter identification would not accept digital data from an IBM system since it is based on a Macintosh system. We feel that the Zonic unit is very well suited to the parameter-identification task.

ROTORDYNAMIC ISSUES

The following two issues were raised during our October discussions:

(a) The lateral rotordynamic characteristics of the tester, and

(b) The possibility of a pitch instability problem with the bearing test assembly.

System Rotordynamics

The compact hollow rotor design of the tester largely precludes any rotordynamic problems. The first free-free bending mode is calculated to be at approximately 200,000 rpm versus an upper running speed limit of 30,000 rpm. Based on TAMU test experience with a larger and heavier rotor, no lateral rotordynamics problems are predicted for this tester.

Pitching/Yawing Instability

Hydrostatic bearings mounted on the TAMU water test stand experienced pitching/yawing instabilities during the initial shakedown of the test facility. The bearings were mounted as shown in figure 9, except the "pitch-stabilizer" cables were not attached.

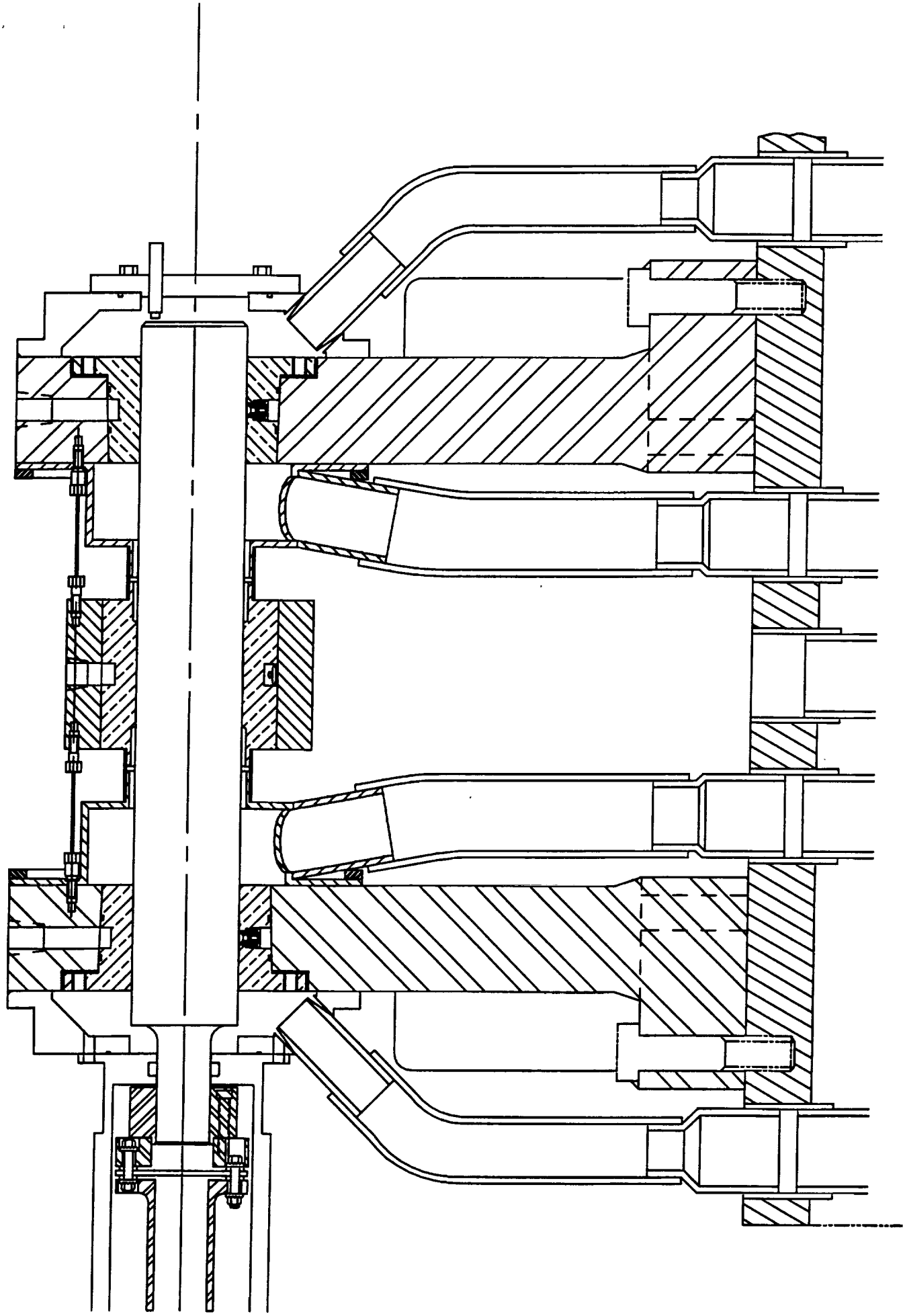

9. TAMU test-bearing assembly

Figure 10a is a spectrum plot of the relative motion between the bearing stator and rotor. The two traces on the plot represent relative motion at opposite ends of the bearing. With a supply pressure of 1000 psi and a rotating speed slightly above 22000 rpm (370 hz), a subsynchronous motion appears around 150 hz . At running speed (370 hz) the front and rear motions are in phase (simple runout or bounce) while at 150 hz they are 180° apart (pitching).

This pitching motion grows rapidly with further increases in rotating speed. Figure 10b shows pitching onset at a lower frequency, around 130 hz, for a decrease in bearing supply pressure to 600 psi. Figures 10a and 10b came from an 0.003 in radial clearance bearing. For a 0.004 in clearance bearing, the rotating speed at which pitching onset occurred was around 17,400 rpm.

This pitching instability limited the testing envelope for the bearing. It could not be fully tested until the "pitch stabilizer" cables shown in figure 9 were attached. These cables eliminated the pitching problem throughout the test-stand operation envelope.

The issue considered here is: Given that the bearing stator of the proposed NASA tester has no direct pitch stabilizers, is conceptually very similar to the initial TAMU tester (which saw limitations due to pitching), will the NASA tester experience pitching instability at some rotating speed?

The initial step taken to analyze the NASA tester was an analysis of the TAMU bearing-tester instability to determine the cause of the observed instability. At the time of the TAMU problems, the available hydrostatic-bearing code would only predict force coefficients not moment coefficients. The present model generates coefficients for the model

$$-\begin{Bmatrix} F_X \\ F_Y \\ M_Y \\ M_X \end{Bmatrix} = [K] \begin{Bmatrix} X \\ Y \\ \alpha_Y \\ \alpha_X \end{Bmatrix} + [C] \begin{Bmatrix} \dot{X} \\ \dot{Y} \\ \dot{\alpha}_Y \\ \dot{\alpha}_X \end{Bmatrix} + [M] \begin{Bmatrix} \ddot{X} \\ \ddot{Y} \\ \ddot{\alpha}_Y \\ \ddot{\alpha}_X \end{Bmatrix} \tag{7}$$

which includes both force and moment coefficients. We have assumed and believe that the observed instability was caused by the additional moment coefficients, and the following analysis was conducted to test this hypothesis.

The motion of the housing assembly was modeled by equations of the form

$$\{ [L] + [M] \}(\ddot{Q}) + [C](\dot{Q}) + \{ [K_s] + [K] \}(Q) = 0 \tag{8}$$

where

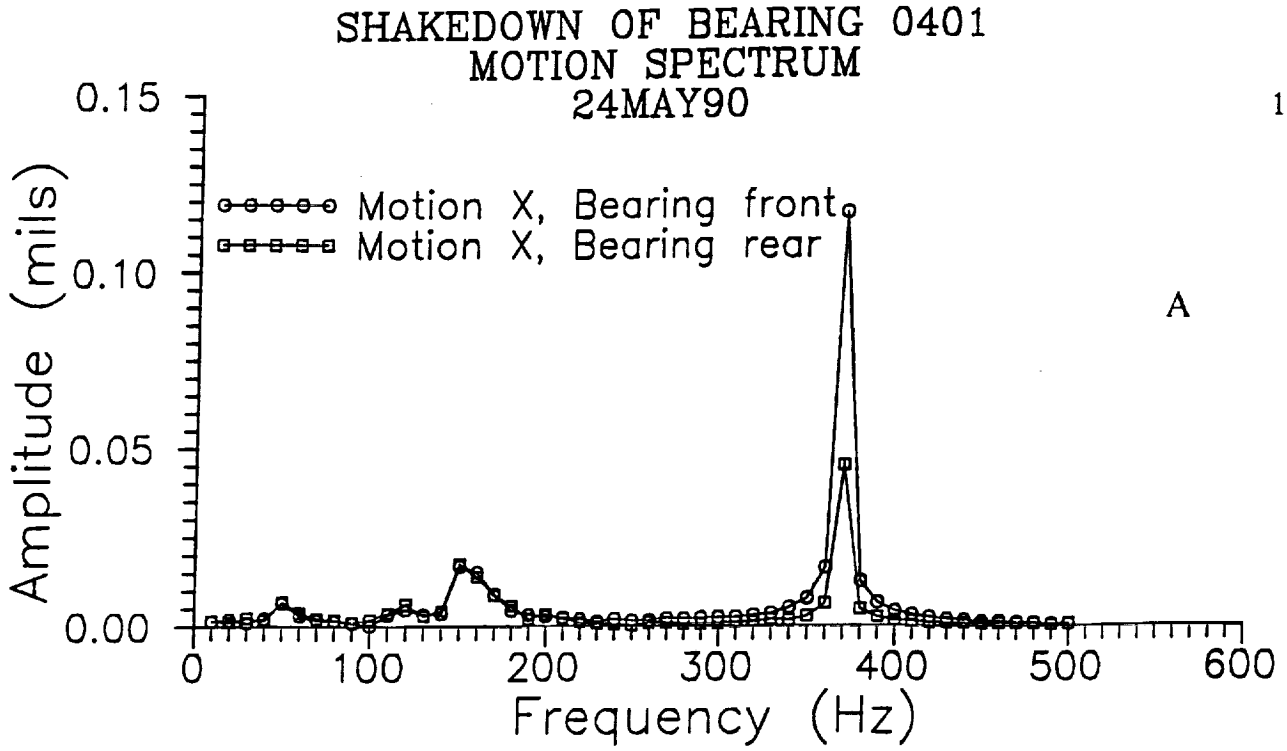

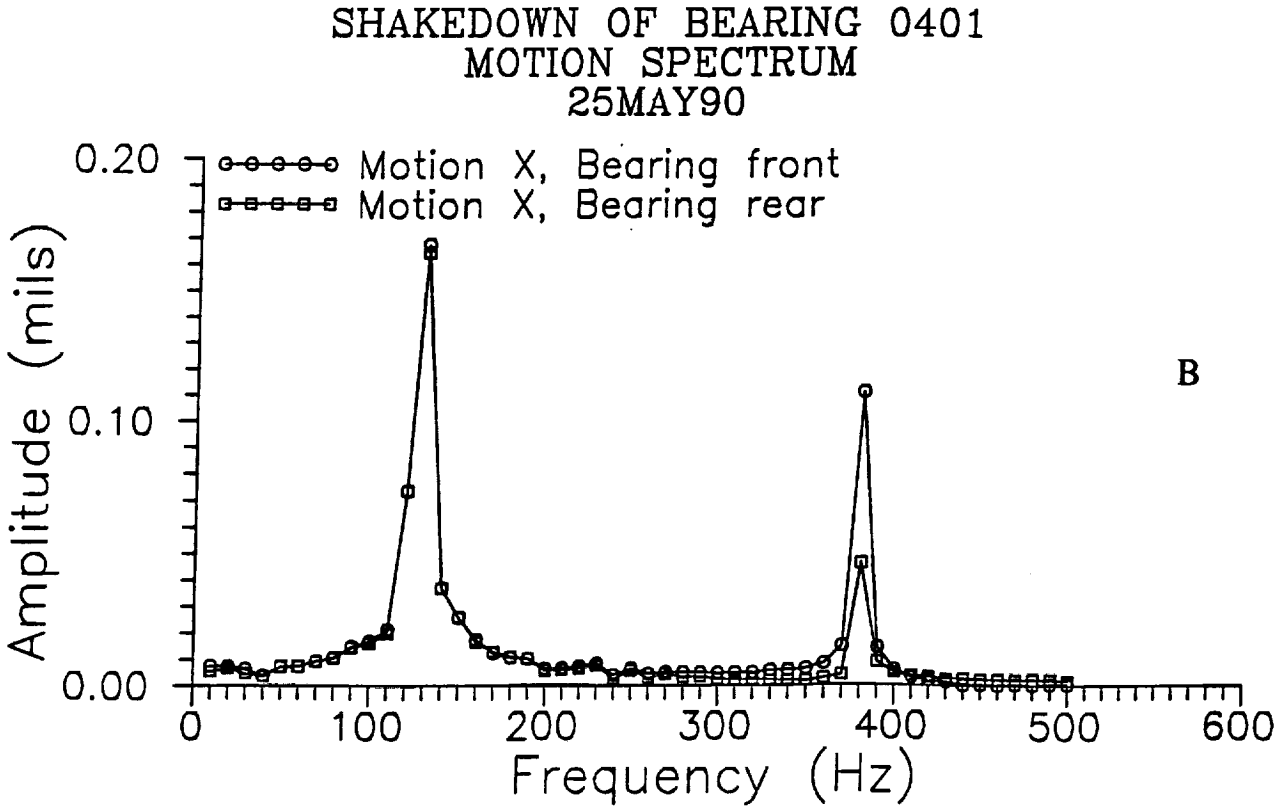

10. Observed rotordynamic instability of a pitch mode during TAMU shake-down test operation; (a) running-speed at 17,400 rpm, subsynchronous motion at 130 Hz, (b) running speed at 22,200 rpm, subsynchronous motion at 150 Hz.

$$[L] = \begin{bmatrix} m & 0 & 0 & 0 & 0 \\ 0 & m & 0 & 0 & 0 \\ 0 & 0 & I & 0 & 0 \\ 0 & 0 & 0 & I & 0 \\ 0 & 0 & 0 & 0 & m \end{bmatrix}, \quad (Q)^T = (X, Y, \alpha_Y, \alpha_X, Z) \quad , \tag{9}$$

where m and I are the bearing-assembly mass and moment of inertia, and $[K_s]$ defines the stiffness matrix for the structure connecting the bearing to "ground." Asymmetry in the structural connection to the test bearing introduce a slight coupling between pitch and yaw and axial motion. Hence, the present model includes the axial displacement Z. The fifth column and row of [M], [C], and [K] which define the bearing contributions are zero. For the initial TAMU configuration, the structure connecting the bearing to ground was just the stingers which connect the test bearing to the shakers. The final TAMU structure includes the pitch-stabilizer cables.

Using Eq.(8) for a model of the TAMU tester with calculated rotordynamic coefficients and beam models for the stingers yielded a prediction of instability at 15,600 rpm versus our actual experience of 17,400 rpm. The predicted pitch frequency of 130 Hz exactly matched our initial test experience. These results strongly support the conclusion that the moment coefficients did, in fact, cause the observed pitch instability.

Figure 11 illustrates the structural and inertial model data used for analysis of the P&W-designed tester. The system was analyzed using calculated bearing data for speeds from 10,000 to 30,000 rpm with supply pressures ranging from 500 to 2000 psi. In proceeding from 10,000 to 30,000 rpm, the radial clearance was reduced from 3.6×10^{-3} in to 3.0×10^{-3} in due to shaft growth. **Calculations were done for LO_2 and LN_2, and no instability is predicted.** These results were surprising to us. They were repeated using the TAMU geometry but NASA operating conditions, and an instability was again predicted. Bearing length appears to be the main difference between the two bearing configurations, with the P&W-designed bearing having L=1.8 in versus L=3 in for the TAMU test bearings. **Note that the present favorable predictions are entirely restricted to the bearing configurations cited by Pelfrey (1993).**

Motion of the Test-Bearing Assembly due to Extraneous Pitch and Yaw Excitation

The sketch of figure 2 shows that the inertia properties of the bearing assembly are not symmetrical about the load axis. The mass center is displaced to the left of this axis by about 0.06 in. Hence the dynamic excitation will create a moment about the mass center of the bearing assembly which will induce pitching and yawing motion of the assembly within the parallel surfaces which are provided to guide the assembly. Pitching and yawing motion will

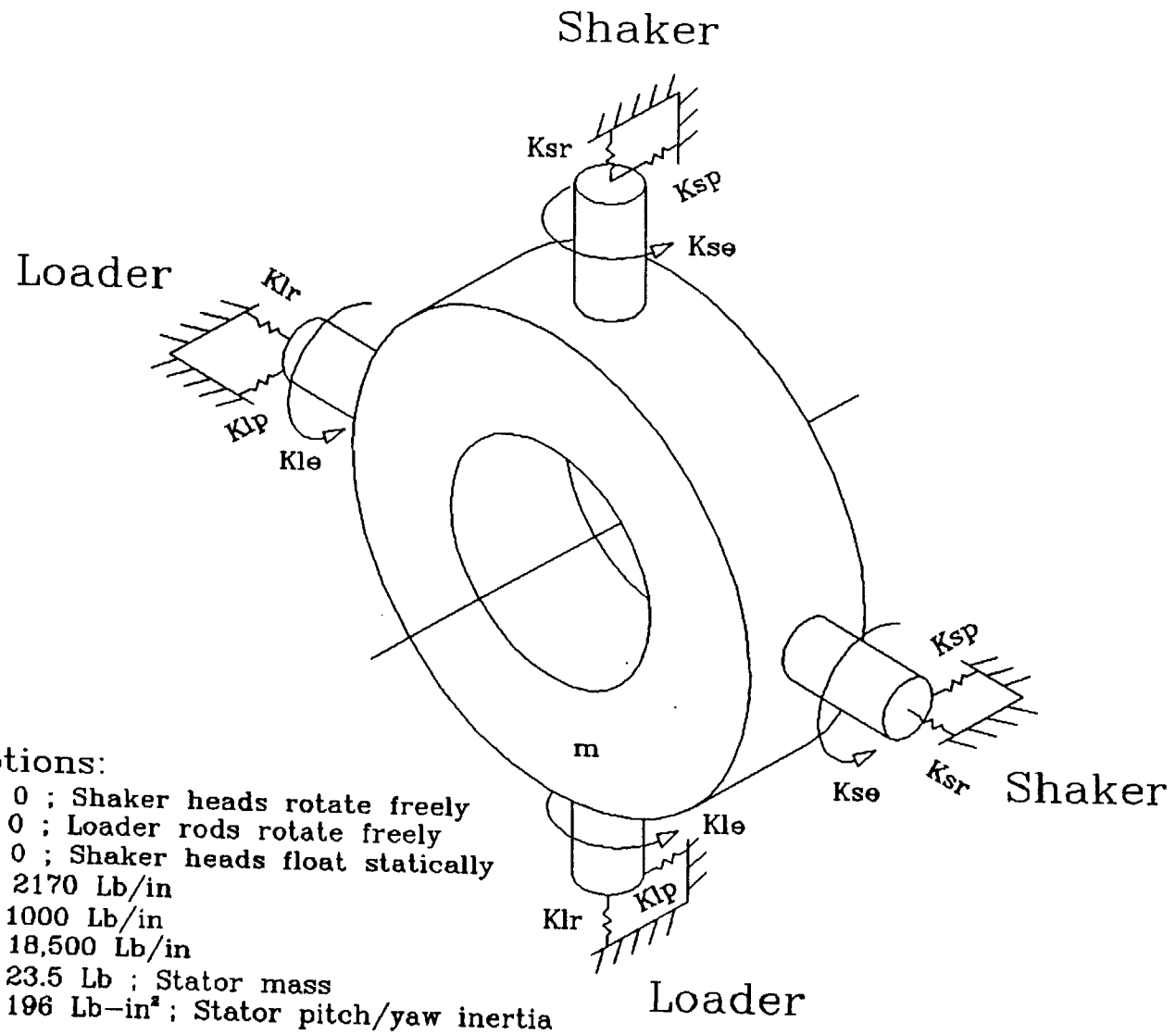

Assumptions:

Kse = 0 ; Shaker heads rotate freely
Kle = 0 ; Loader rods rotate freely
Ksr = 0 ; Shaker heads float statically
Ksp = 2170 Lb/in
Klr = 1000 Lb/in
Klp = 18,500 Lb/in
m = 23.5 Lb ; Stator mass
I = 196 Lb–in^2 ; Stator pitch/yaw inertia

11. Structure and stiffness model for the P&W tester.

in turn cause the outer surfaces of the bearing assembly to oscillate axially. The axial clearance range of the assembly between the parallel surfaces is C_z=.5 x 10^{-3}/2.5 x 10^{-3} in. The weight of the assembly will cause it to rest on the lower surface creating Coulomb friction forces as discussed in the section on Extraneous Load Paths. Induced motion of the assembly involving time varying contact forces and Coulomb-friction forces is beyond the scope of this study; however, to provide some order-of-magnitude analysis for this motion, simulations were conducted to see how large the induced axial motion would be (without contact).

Displacing the mass center axially to the right of the line of action of the applied force by the distance b_Z means that the equations of motion for the body becomes

$$\begin{aligned} m\ddot{X} + mb_Z\ddot{\alpha}_Y &= \Sigma F_X \\ m\ddot{Y} - mb_Z\ddot{\alpha}_X &= \Sigma F_Y \\ I\ddot{\alpha}_Y + mb_Z\ddot{X} &= \Sigma M_Y \\ I\ddot{\alpha}_X - mb_Z\ddot{Y} &= \Sigma M_X \\ m\ddot{Z} + b_Z m(\dot{\alpha}_X^2 + \dot{\alpha}_Y^2) &= \Sigma F_Z \end{aligned} \tag{10}$$

For these equations, the X and Y axes about which moments are taken continue to coincide with the axes of applied forces.

Eq.(8) is now stated

$$\{ [\bar{L}] + [M] \}(\ddot{Q}) + [C](\dot{Q}) + \{ [K_s] + [K] \}(Q) = (F) \tag{11}$$

where

$$[\bar{L}] = \begin{bmatrix} m & 0 & mb_Z & 0 & 0 \\ 0 & m & 0 & -mb_Z & 0 \\ mb_Z & 0 & I & 0 & 0 \\ 0 & -mb_Z & 0 & I & 0 \\ 0 & 0 & 0 & 0 & m \end{bmatrix}, \quad (F) = \begin{bmatrix} fs_x(t) \\ fs_y(t) \\ 0 \\ 0 \\ -b_Z m(\dot{\alpha}_X^2 + \dot{\alpha}_Y^2) \end{bmatrix} \tag{12}$$

Eq.(11) is integrated with zero initial conditions using two cycles of measured TAMU excitation data.

The axial motion is obtained via

$$\tilde{Z} = Z + \alpha R_{MAX} \quad , \quad \alpha = \sqrt{\alpha_X^2 + \alpha_Y^2}$$

where, R_{MAX} = 3.625 in is the maximum radius of the bearing assembly. This definition yields a prediction of only positive motion; however, diagonally across from the position that is moving in the positive Z direction, the "backside" of the assembly is moving about the same amount in the -Z direction.

Simulations with LO_2 and LN_2 yielded approximately the same magnitudes for $\tilde{Z}$. The results are very nearly proportional to b_Z. Simulations are shown in figure 12 for a high-speed, high-pressure condition. Note that the radial X motion amplitude within the bearing is on the order of 10% of the bearing clearance; $C_r = 3.0 \times 10^{-3}$ in. Peak axial motion is approximately 7% of the minimum axial clearance, and 1.4% of the maximum axial clearance. Figure 13 illustrates results for a low speed, low pressure condition. The excitation forces have been scaled down (markedly) to continue yielding radial motion on the order of 10% of the radial bearing clearance; $C_r = 3.6 \times 10^{-3}$ in. The resultant peak axial motion is on the order of 10% of the minimum axial clearance and 2% of the maximum axial clearance.

The present simulations do not speak to the magnitude of reaction forces occasioned by forced contact with the wall. They do indicate that intermittent contact will occur, complicating further the question of the influence of Coulomb-friction forces on measured uncertainties. Note that the induced pitching motion will tend to yield a point contact at the outer radius of the bearing assembly during sliding motion.

The present results also suggest another complication due to forced pitching and yawing motion; namely, the motion transducers are attached to the bearing assembly and will "measure" induced pitch and yaw motion in addition to the intended radial motion. The sensors are located at approximately Z_s = 1.345 in to the right of the X and Y axes. The total motion is

$$\begin{aligned} \tilde{X} &= X + \alpha_Y Z_s \\ \tilde{Y} &= Y - \alpha_X Z_s \end{aligned} \qquad (13)$$

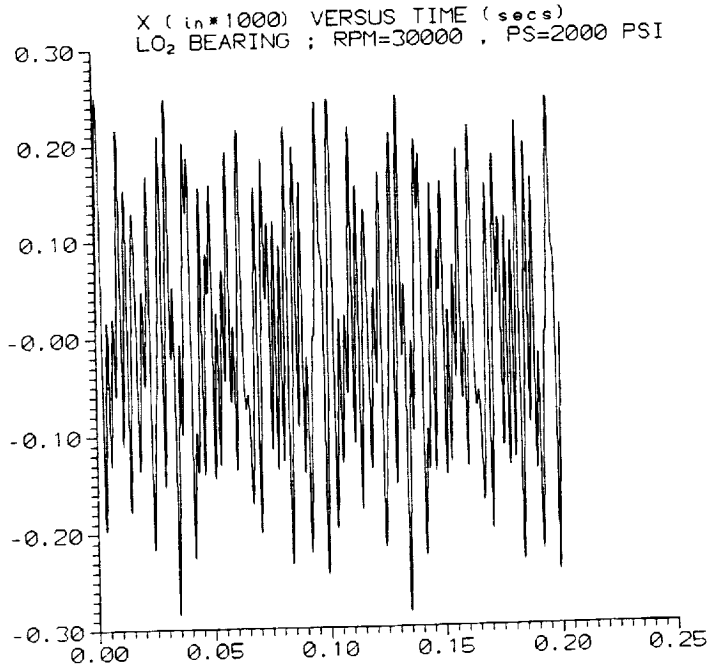

A

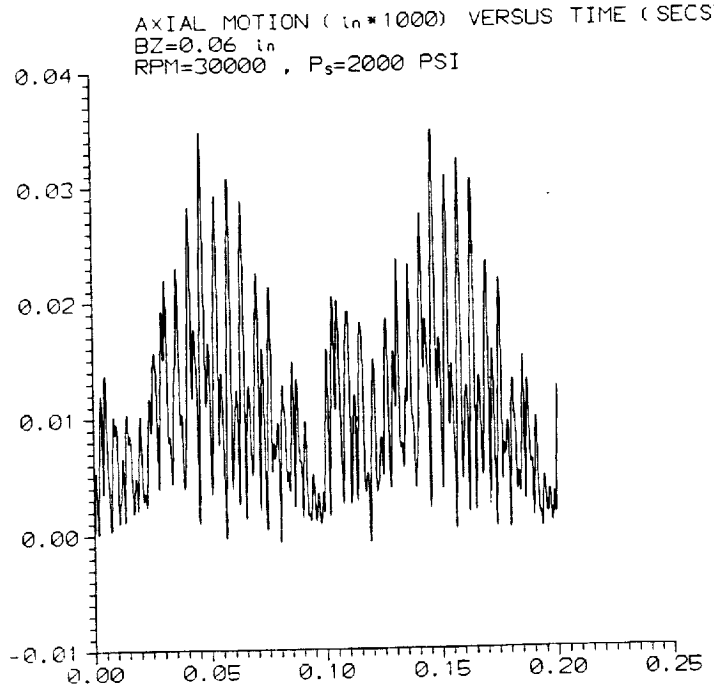

B

12. Predicted response of the test-bearing assembly during $fs_x(t)$ excitation with LO_2 as a test fluid and b_Z = 0.06 in, ω = 30,000 rpm and P_s = 2000 psi; (a) radial motion, (b) induced axial motion.

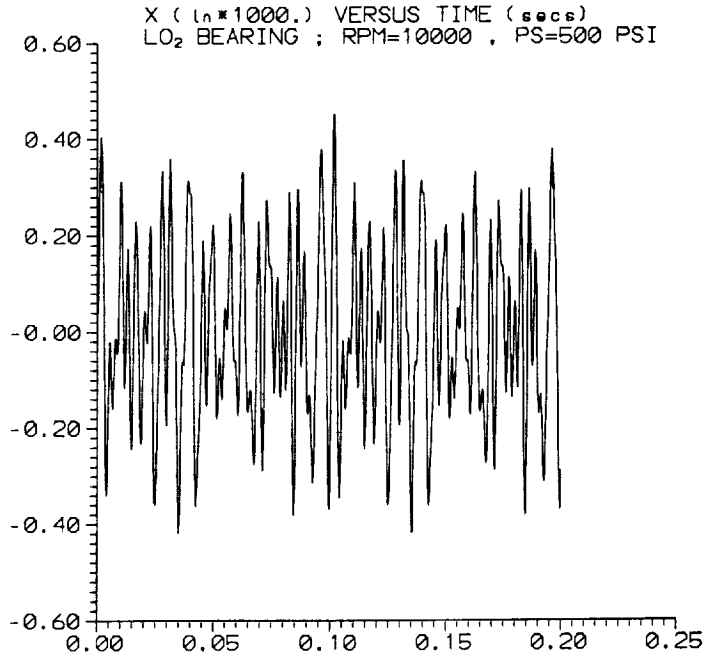

A

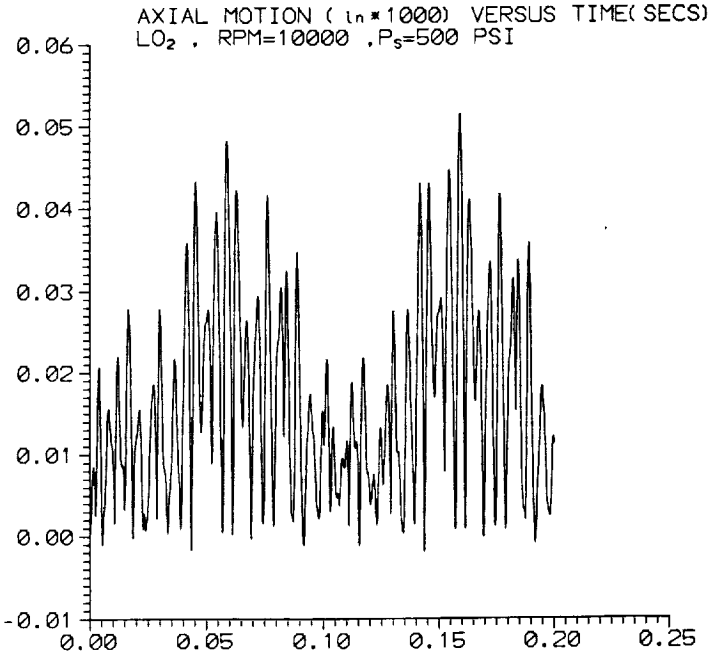

B

13. Predicted response of the test-bearing assembly during $fs_x(t)$ excitation with LO_2 as a test fluid and b_Z = 0.06 in, ω = 10,000 rpm, and P_s = 500 psi; (a) radial motion, (b) induced axial motion.

The terms $\alpha_Y Z_s$ and $\alpha_X Z_s$ are errors in the measured radial displacement of the bearing. For predominant *X* excitation, the largest motion and error are in the *X* direction. Figure 14 provides the induced error for the two excitation cases of figures 12 and 13. The error is larger for the high-speed, high-pressure case because the excitation force is larger. The average error is about 4% for the high-speed and high-pressure case and about .5% for the low-speed and low-pressure case.

The predicted problems due to the mass center offset are not terribly alarming; however, they are an unneeded and avoidable complication. **We recommend that the parts be redesigned to move the mass center into alignment with the axes of the applied forces.**

UNCERTAINTY PREDICTIONS

Uncertainty predictions for rotordynamic coefficients are based on specifications of individual measurement components. The measurement components which impact the uncertainty of rotordynamic coefficients are the force transducers on the shaker heads, the accelerometers, and the motion transducers. Data are available to estimate errors in the force and acceleration measurements, and static calibration data are available for the motion transducers at cryogenic temperatures. Unfortunately, phase-error data are not available for the motion transducers. However, P&W personnel have expressed high confidence in the frequency-response characteristics of the motion transducers. Assuming that the motion transducers selected for the NASA test rig work as well as the TAMU transducers, the principal changes in uncertainty values between those calculated for TAMU and the NASA test rig will arise due to increased supply pressures (from 1000 to 2000 psi) and increased running speeds (from 24,650 to 30,000 rpm). Hence, to arrive at estimates for uncertainties for rotordynamic coefficients obtained from the NASA test rig, data were extrapolated from the TAMU test rig. Estimated uncertainty values are provided below:

Coefficient	**Estimated Uncertainty (%)**
K_{XX}, K_{YY}	1.3
K_{XY} , K_{YX}	1.7
C_{XX}, C_{YY}	2.9
C_{XY}, C_{YX}	21
M_{XX}, M_{YY}	27

Table 1: Projected uncertainties in rotordynamic coefficients for the NASA test rig operating at 30,000 rpm and 2000 psi.

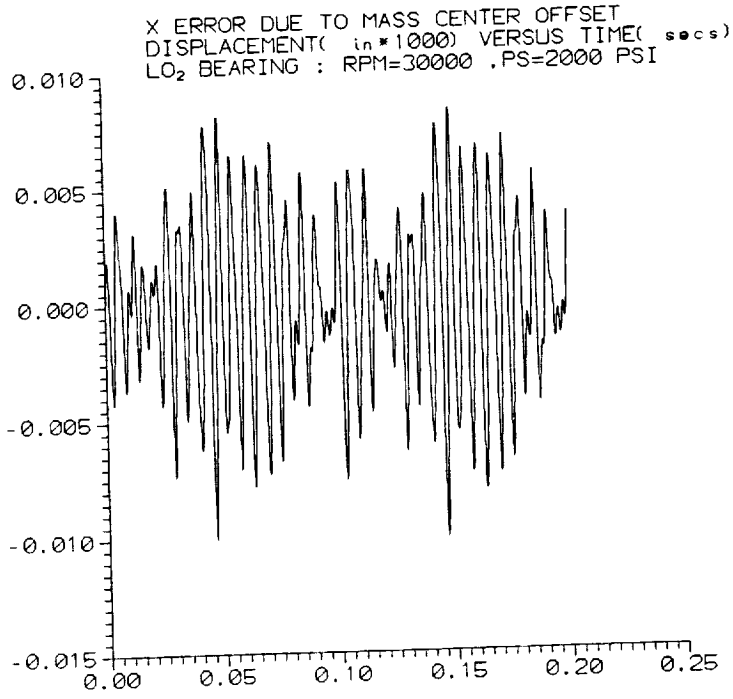

A

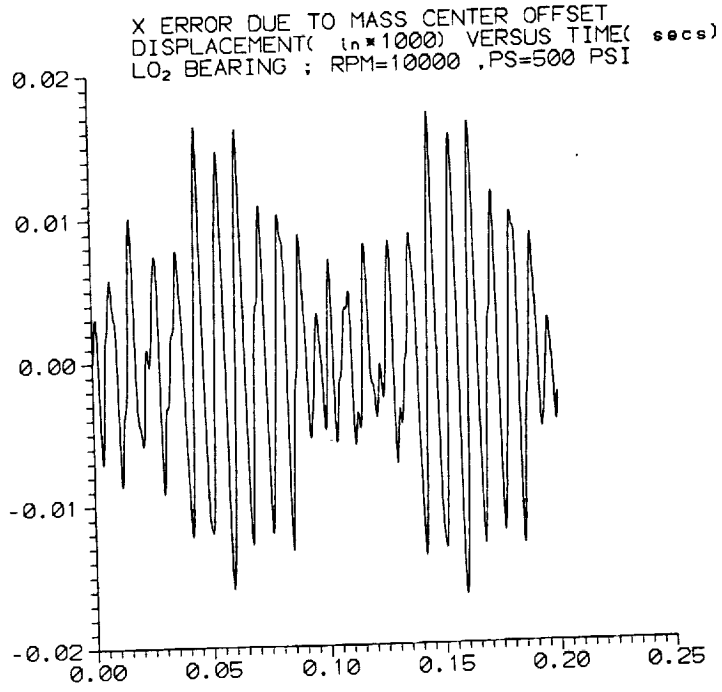

B

14. Error in X measurements with $fs_x(t)$ excitation due to induced pitching motion; (a) ω = 30,000 rpm, and P_s = 2000 psi, and (b) ω = 10,000 rpm, and P_s = 500 psi.

SUMMARY AND RECOMMENDATIONS

Summary

Generally speaking, the P&W test rig is a sound and well designed system. It copies many of the successful features which have been demonstrated in the TAMU tester, Childs and Hale (1993). This study has raised numerous issues, most of which have been satisfactorily resolved by either analysis or hardware modifications. The following unresolved issues remain which can adversely impact the effectiveness of the tester:

(a) Most of the remaining extraneous load paths presented by the design can be calibrated by dry shake testing. However, the influence of the static seals and the influence of Coulomb friction remain unresolved. The influence of static seals can be calibrated by a dry shake test of the bearing with the orifices plugged using gaseous N_2. The Coulomb-friction forces arising at parallel guide surfaces can not be calibrated out and represents a continuing uncertainty in measured damping and mass coefficients. A redesign using hydrostatic centering pads would eliminate the problem. However, the present calculated errors due to Coulomb friction may well be acceptable.

(b) Static data cited by P&W for the displacement probes to be used in the tester are excellent. Unfortunately, dynamic data for amplitude and phase are not available for these transducers at cryogenic temperatures. **This absent data represents the central uncertainty in deciding whether the tester will work effectively or at all in producing rotordynamic coefficients.**

(c) Static load requirements are met marginally by the present loaders. A single loader, operating within manufacturer's recommendations will only achieve an on-axis eccentricity ratio of 0.424 with LO_2 and 0.456 with LN_2.

(d) The pressures under bearing recesses and extending out to the bearing edges will cause small but finite deflections on the present hollow-shaft design which can not be accounted for in the present bearing codes and will not be present in solid-shaft applications. A rough estimate of the local displacements indicates that they can amount to 7% of the radial clearance.

(e) The static pressure measurements can introduce a capacitance connection to the recesses. Capacitances have been demonstrated to cause a major change in rotordynamic behavior. At a presentation of final results from this study on October 28, 1994, we were informed that P&W proposed to resolve this issue by placing acutator valves in the pressure tap lines between the bearings and the pressure read outs. The valves would be closed during dynamic testing but otherwise open. This is an attractive proposal, providing that the valves are within the tester and at cryogenic temperatures, such that no gas pocket forms within the lines between the valves and the bearing recesses.

(f) The effectiveness of the parameter identification hardware and software remains unvalidated by real data.

(g) To our surprise, no pitching and yawing instability was predicted for the P&W tester using the bearing and operating conditions cited by Pelfrey (1993)!

(h) The offset of the mass center of bearing test assembly will induce pitching and yawing motion of the bearing during test excitation. Consequently, axial motion at the outer radius of the bearing will cause a "rattling" intermittent contact at the guide surfaces. Further, the pitching and yawing will cause an error in the radial displacement measurements on the order of 4%.

Recommendation

Based on the results cited, the following recommendations are offered:

(a) Consider a redesign of the tester to provide a positive friction-free guide to eliminate Coulomb friction forces. Three hydrostatic pads on each side of the bearing would eliminate this problem.

(b) Conduct or commission tests to demonstrate the dynamic characteristics of the motion transducers in LO_2 and LN_2.

(c) Validate the parameter identification system for rotordynamic coefficients. Tests will resume at TAMU during 1995, and the Zonic unit could be used to collect our data for validation.

(d) Redesign the unit to move the mass center of the test-bearing assembly into coincidence with forces axes.

REFERENCES

Childs, D., and Hale, K., (1993), "A Test Apparatus and Facility to Identify the Rotordynamic Coefficients of High-Speed Hydrostatic Bearings," *ASME Trans., Journal of Tribology,* April, Vol. 116, pp. 337-344.

Goodwin, M.J., Roach, M.P., and Penny, J.E.T., (1988), "An Analysis of Combined Squeeze-Film and Variable Stiffness Hydrostatic Bearings, and Their Use in Aircraft Engine Vibration Control," *Vibration in Rotating Machinery*, IMechE, pp. 85-91.

Pelfrey, P., (1993), "NASA Hydrostatic Bearing Rig Bearing Design," Internal P&W memorandum to J. Justak, 4 November 1993.

Rouvas, C., and Childs, D., (1993), "A Parameter Identification Method for the Rotordynamic Coefficients of a High Reynolds Number Hydrostatic Bearing," *ASME Trans., Journal of Vibration and Acoustics,* July, Vol. 115, pp. 264-270.